Journal of Pharmaceutical Analysis 6 (2016) 56–63

HOSTED BY

Contents lists available at ScienceDirect

Journal of Pharmaceutical Analysis

journal homepage: www.elsevier.com/locate/jpa
www.sciencedirect.com

Original Article

Spectroscopic analysis on the binding interaction of biologically active pyrimidine derivative with bovine serum albumin ☆

Vishwas D. Suryawanshi, Laxman S. Walekar, Anil H. Gore, Prashant V. Anbhule, Govind B. Kolekar *

Fluorescence Spectroscopy Research Laboratory, Department of Chemistry, Shivaji University, Kolhapur 416 004, Maharashtra, India

ARTICLE INFO

Article history:
Received 22 November 2014
Received in revised form
11 July 2015
Accepted 14 July 2015
Available online 15 July 2015

Keywords:
Bovine serum albumin
Fluorescence spectroscopy
Pyrimidine derivative
Binding interaction
Fluorescence resonance energy transfer (FRET)

ABSTRACT

A biologically active antibacterial reagent, 2–amino-6-hydroxy–4–(4-N, N-dimethylaminophenyl)-pyrimidine-5-carbonitrile (AHDMAPPC), was synthesized. It was employed to investigate the binding interaction with the bovine serum albumin (BSA) in detail using different spectroscopic methods. It exhibited antibacterial activity against *Escherichia coli* and *Staphylococcus aureus* which are common food poisoning bacteria. The experimental results showed that the fluorescence quenching of model carrier protein BSA by AHDMAPPC was due to static quenching. The site binding constants and number of binding sites ($n \approx 1$) were determined at three different temperatures based on fluorescence quenching results. The thermodynamic parameters, enthalpy change (ΔH), free energy (ΔG) and entropy change (ΔS) for the reaction were calculated to be 15.15 kJ/mol, −36.11 kJ/mol and 51.26 J/mol K according to van't Hoff equation, respectively. The results indicated that the reaction was an endothermic and spontaneous process, and hydrophobic interactions played a major role in the binding between drug and BSA. The distance between donor and acceptor is 2.79 nm according to Förster's theory. The alterations of the BSA secondary structure in the presence of AHDMAPPC were confirmed by UV–visible, synchronous fluorescence, circular dichroism (CD) and three-dimensional fluorescence spectra. All these results indicated that AHDMAPPC can bind to BSA and be effectively transported and eliminated in the body. It can be a useful guideline for further drug design.

1. Introduction

Protein, one of the most important bioactive molecules, is related to alimentation, immunity and metabolism. The content of proteins in body fluid can be used as a vital index for the clinical diagnosis and health evaluation; therefore, the direct determination of protein is significant in life sciences, clinical medicine and chemical investigation. The interaction between bio-macromolecules and drugs has attracted great interest for several decades [1–3] and many researches have been focused on two central questions about proteins: what are the determinant factors that influence the protein structures and functions, and how does a factor affect their biological activity [4,5]. Serum albumin (SA), the main protein in the blood plasma acting as the transporter and disposition of many drugs, has been frequently used as a model protein for investigating protein folding and ligand binding mechanism. In this regard, bovine serum albumin (BSA) has been studied extensively, partly because of its structural homology with human serum albumin (HSA) [6,7]. BSA is composed of three linearly arranged and structurally homologous sub-domains. It has two tryptophan residues that possess intrinsic domains (I–III) and each domain in turn is the product of two fluorescence: Trp-134, which is located on the surface of sub-domain IB, and Trp-212, located within the hydrophobic binding pocket of sub-domain IIA [8,9]. The binding sites of BSA for endogenous and exogenous ligands may be in these domains and the principal regions of drugs binding sites of albumin are often located in hydrophobic cavities in sub-domains IIA and IIIA. So-called sites I and II are located in subdomain IIA and IIIA of albumin, respectively.

Pyrimidine moiety is one of the important classes of N-containing heterocycles widely used as key building blocks for pharmaceutical agents. It exhibits a wide spectrum of pharmacophore such as bactericidal, fungicidal, analgesic, anti-hypertensive and anti-tumor agents [10–13]. In addition, preclinical data from literature survey indicate continuing research in polysubstituted pyrimidine as potential anti-tumor agents [14]. 2-amino-6-hydroxy-4-(4-N,N-dimethylaminophenyl)-pyrimidine-5-carbonitrile (AHDMAPPC), a pyrimidine derivative, and its analogs possessing

☆ Peer review under responsibility of Xi'an Jiaotong University.

* Corresponding author. Fax: +91 0231 2692333
E-mail address: gbkolekar@yhaoo.co.in (G.B. Kolekar).

http://dx.doi.org/10.1016/j.jpha.2015.07.001

anti-bacterial activity were synthesized in our laboratory [15]. AHDMAPPC was synthesized by three-component condensation of aromatic aldehyde, ethyl cyanoacetate and guanidine hydrochloride in ethanol under alkaline medium.

Protein–drug interaction plays an important role in pharmacokinetics and pharmacodynamics. In a series of methods concerning the interaction of drugs and protein, fluorescence techniques are great aids in the study of interactions between drugs and serum albumin because of their high sensitivity, rapidity, and ease of implementation [16]. The aim of the present investigation was to study the affinity of pyrimidine derivative (AHDMAPPC) for BSA using UV–visible and fluorescence spectroscopy to understand the carrier role of serum albumin for such compound in the blood under physiological conditions. Significantly, the determination and understanding of drug interacting with serum albumin are important for the therapy and design of drug [17]. Knowledge of the interaction and binding of BSA may open new avenues for the design of the most suitable pyrimidine derivatives. All the experimental results clarify that AHDMAPPC can bind to BSA and be effectively transported and eliminated in body, which can be a useful guideline for further drug design.

In this paper, we have studied *in vitro* interaction of AHDMAPPC with BSA by the fluorescence quenching method. The binding constants were obtained at different temperatures in the medium of Tris–HCl (pH 7.4) buffer solution. The binding sites and main sorts of binding forces have been suggested. In addition, the conformational changes of BSA were discussed on the basis of UV–visible spectroscopy, synchronous fluorescence (SF), circular dichroism (CD) and three-dimensional spectroscopy.

2. Materials and methods

2.1. Materials

BSA (essentially fatty acid free) was purchased from Hi-Media Chemical Company (Mumbai, India) and its molecular weight was assumed to be 66, 463 to calculate the molar concentrations. All BSA solutions ($C_{BSA}=2.0\times10^{-5}$ M) were prepared in a pH 7.4 buffer solution and the stock solution was kept in the dark at 4 °C. Tris–HCl (0.1 M) buffer solution containing NaCl (0.1 M) was used to keep the pH of the solution at 7.4. A dilution of the BSA stock solution in Tris–HCl buffer solution was prepared immediately before use. The stock solution of AHDMAPPC (synthesized) was prepared in (5:95, v/v) ethanol water mixture. Dissolution of the compound was enhanced by sonication in an ultrasonic bath (Spectra Lab Model UCB-40). All chemicals were of analytical reagent grade and were used without further purification. Double distilled water was used throughout. In order to simulate human body fluid surroundings and to get the best sensitivity, Tris–HCl solution (pH 7.4) was chosen as the buffer solution in this work.

2.2. Equipment and spectral measurements

All fluorescence emission spectra were recorded on PC based Spectrofluorometer (JASCO Japan FP-750) equipped with an Xenon lamp and 1.0 cm quartz cell. Fluorescence emission spectra were recorded at three different temperatures, 300, 310 and 320 K. Excitation and emission slit width was fixed to 10 nm. An excitation wavelength of 280 nm was chosen, because it is exclusively due to the intrinsic Tryptophan (Trp) fluorophore. The UV–visible absorption spectra were measured at room temperature on a Shimadzu UV–3600 UV–vis–NIR Spectrophotometer equipped with a 1.0 cm quartz cell. The wavelength range was from 250 to 450 nm. All pH values were measured by a digital pH-meter with magnetic stirrer (Equip-Tronics EQ-614A). For synchronous fluorescence measurements, the excitation range was 260 – 360 nm, and $\Delta\lambda$ was set at 15 and 60 nm. Circular dichroism (CD) spectra were measured with a Jasco J-815 Spectropolarimeter (Jasco, Tokyo, Japan) at room temperature over the wavelength range of 200–250 nm using a 1.0 cm quartz cell. The three-dimensional fluorescence spectra were performed under the following conditions: the emission wavelength was recorded between 250 and 500 nm; the initial excitation wavelength was set to 250 nm with increment of 10 nm for each scanning curve; other scanning parameters were identical to those of the fluorescence emission spectra. Appropriate blanks corresponding to the buffer were subtracted to correct the absorbance or fluorescence background.

3. Results and discussions

3.1. Fluorescence quenching studies of BSA by pyrimidine derivative (AHDMAPPC)

Protein is considered to have intrinsic fluorescence mainly originating from the tryptophan (Trp), tyrosine (Tyr), and phenylalanine (Phe) residues [18]. When it interacts with other compounds, its intrinsic fluorescence often changes with the ligand's concentration. Consequently, fluorescence can be regarded as a technique for measuring the mechanism of interactions between ligands and proteins [19]. The concentration of BSA solutions was stabilized and the concentrations of AHDMAPPC were varied in the experiment. Fluorescence spectra of BSA, after the addition of AHDMAPPC, were recorded upon excitation at 280 nm and 300 K, as illustrated in Fig. 1. It was observed that BSA exhibited a strong fluorescence emission band at 347 nm. The fluorescence intensities of BSA reduced gradually with increasing AHDMAPPC concentrations, and a blue shift was also observed, which suggests that the fluorescence chromophore of serum albumin is placed in a more hydrophobic environment after the addition of AHDMAPPC. The fluorescence quenching effect was due to the formation of non-fluorescent complex [20]. Fluorescence quenching is the decrease of the fluorescence quantum yield from a fluorophore induced by a variety of molecular interactions, such as excited-state reactions, energy transfer, ground-state complex formation, and collisional quenching. The quenching mechanisms are usually classified as dynamic quenching and static quenching, which can be distinguished by their different dependence on temperature and viscosity [21]. Since higher temperatures result in large diffusion coefficients for dynamic quenching, the quenching constants are expected to increase with increasing temperature. In contrast, a higher temperature may bring about the decrease in the stability of the complexes, resulting in a lower quenching constant for the static quenching.

3.2. Quenching mechanism analysis

To further elucidate the quenching mechanism of BSA induced by pyrimidine derivative, the fluorescence quenching data were analyzed with the Stern–Volmer equation [22].

$$F_0/F = 1 + k_q\tau_0[Q] = 1 + K_{SV}[Q] \quad (1)$$

where F_0 and F are the relative fluorescence intensities in the absence and presence of quencher respectively, $[Q]$ is the concentration of quencher, K_{SV} the Stern–Volmer dynamic quenching constant, k_q the bimolecular quenching rate constant and τ_0 the average lifetime of the fluorophore in the excited state usually for a biomacrolecule10^{-8} s [23–25]. The formation of complex was further confirmed from the values of quenching rate constants k_q,

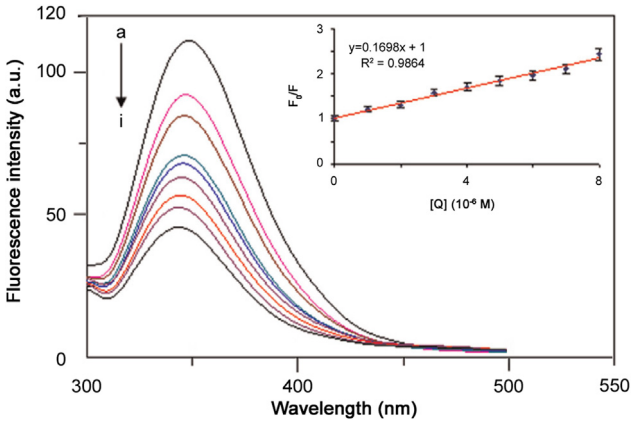

Fig. 1. The fluorescence quenching spectra of BSA in the presence of AHDMAPPC $C_{BSA}=2.0\times10^{-5}$ M; $C_{AHDMAPPC}(10^{-6}$ M) (a–i): 0, 1.0, 2.0, 3.0, 4.0, 5.0, 6.0 7.0, 8.0, (T=300 K, pH=7.4, λ_{ex}=280 nm).

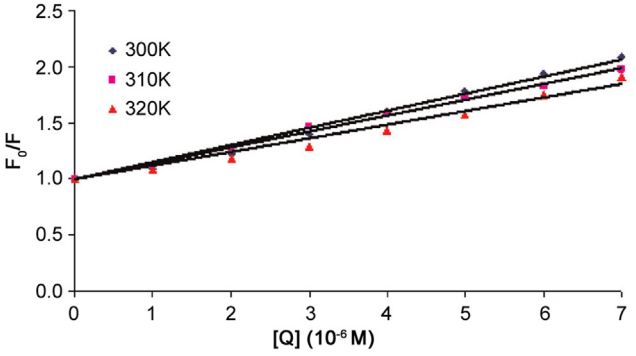

Fig. 2. Stern–Volmer plots describing BSA quenching caused by AHDMAPPC at three different temperatures. C_{BSA} is the same as that in Fig. 1.

Table 1
Stern–Volmer quenching constants and bimolecular quenching rate constants for the interaction of AHDMAPPC with BSA at various temperatures.

T (K)	K_{sv} (10^{-5}, L/mol)	k_q (10^{-13}, L/mol s)	R
300	1.6292	1.6292	0.9968
310	1.4102	1.4102	0.9978
320	1.3135	1.3135	0.9928

R is the correlation coefficient.

$$k_q = K_{SV}/\tau_0 \quad (2)$$

Fig. 2 shows the plot of F_0/F for BSA versus [AHDMAPPC] at 300 K, 310 K and 320 K. Linear fittings of the experimental data obtained afford K_{SV} and k_q (Table 1). The plots showed that within the investigated concentration, the results exhibited a good linear relationship. Table 1 shows that K_{SV} values were inversely correlated with temperatures, which suggests that the fluorescence quenching of BSA was initiated by the formation of ground-state complex. For dynamic quenching, the maximum scattering collision quenching constant of various quenchers is (2.0×10^{10} L/mol s) [26]. The results showed that the value of k_q was much greater than 2.0×10^{10} L/mol s, which indicated that the probable quenching mechanism of fluorescence of BSA by AHDMAPPC is not caused by dynamic collision but from the formation of a complex. It is well known that the Stern–Volmer equation is fit for both dynamic and static quenching mechanism. Nevertheless, the Stern–Volmer slope (K_{SV}) is expected to depend on the concentration of BSA in a static quenching process, whereas the slope

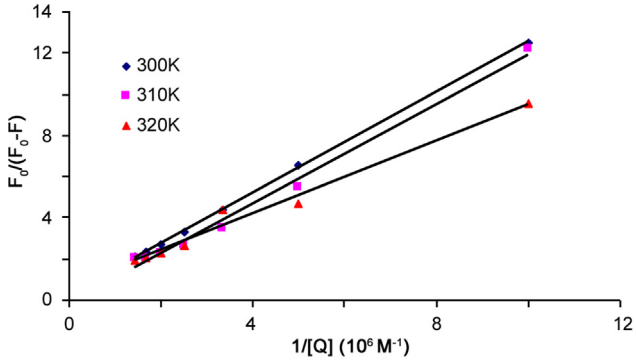

Fig. 3. Modified Stern–Volmer plot for the binding of BSA–AHDMAPPC.

does not change at any concentration of BSA in a dynamic process. It again indicates that the quenching arises from the complex formation rather than a dynamic process. The fluorescence data were further examined using modified Stern–Volmer equation [27]:

$$F_0/\Delta F = [1/f_a K_a][1/[Q]] + 1/f_a \quad (3)$$

where f_a is the fraction of the initial fluorescence that is accessible to quencher; K_a is the Stern–Volmer quenching constant of the accessible fraction and $[Q]$ is the concentration of quencher. Fig. 3 displays the modified Stern–Volmer plots; the dependence of $F_0/\Delta F$ on the reciprocal values of the quencher concentration $[Q]^{-1}$ is linear. The plots showed that within the investigated concentration, the results exhibited a good linear relationship, which again confirms that quenching mechanism between pyrimidine derivative and BSA belongs to the static quenching.

3.3. Evaluation of the binding constant and binding site

The usefulness of the drugs as therapeutic agents is basically dependent on their binding ability that can also influence the drug stability and toxicity during their chemotherapeutic process. In addition, the drug–protein complex may be considered as an excellent miniature model for gaining insights into the general drug–protein interaction. To see the binding interaction between AHDMAPPC and serum albumin, the binding constant values were determined from the fluorescence intensity data.

When small molecules bind independently to a set of equivalent sites on a macromolecule, the equilibrium between free and bound molecules is given by the following equation [28]:

$$\log\frac{(F_0-F)}{F} = \log K + n\log[Q] \quad (4)$$

Thus, for a static quenching interaction, the binding constant

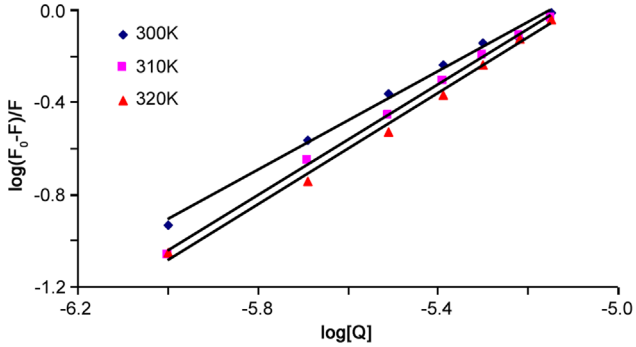

Fig. 4. The plots of $\log(F_0-F)/F$ versus $\log[Q]$ at three different temperatures. C_{BSA} and $C_{AHDMAPPC}$ are the same as those in Fig. 1.

Table 2
Binding constants (K) and the number of binding sites (n) of competitive experiment of AHDMAPPC–BSA system.

T (K)	K (10^{-5}, L/mol)	n	R
300	9.6694	1.0657	0.9964
310	12.8262	1.1005	0.9994
320	14.4249	1.2066	0.9971

R is the correlation coefficient.

(K) and the number of binding sites (n) per BSA molecule can be determined at physiological pH 7.4, where F_0, F, and [Q] are the same as those in Eq. (1). A plot of log [$(F_0 - F)/F$] versus log [Q] (Fig. 4) gives a straight line, whose slope equals n and the intercept on the Y-axis equals log K. The values of K and n at 300, 310 and 320 K are listed in Table 2. The values of n for serum albumin, BSA, are approximately equal to one, indicating that there is one binding site in BSA for pyrimidine derivative during their interaction. The binding strength of the drug to BSA is the main factor in its availability to diffuse from the circulatory system to target [29]. Most ligands are bound reversibly and exhibit moderate affinities for protein [binding constants in the range $(1–15) \times 10^4$ L/mol] [30]. So the K values show that the binding between AHDMAPPC and BSA is moderate, which indicates that a reversible AHDMAPPC–BSA complex formation and AHDMAPPC can be stored and carried by BSA.

3.4. Thermodynamic parameters and binding forces

The interaction forces between a small organic molecule and a biological macromolecule mainly consist of four types: hydrophobic interactions, hydrogen bonding, van der Waals forces, and electrostatic interactions. Ross and Subramanian have characterized the signs and magnitudes of the thermodynamic parameters (ΔH and ΔS) associated with various individual kinds of interaction that may take place in protein association process [31]. That is, if $\Delta H > 0$ and $\Delta S > 0$, the main force is hydrophobic interaction. If $\Delta H < 0$ and $\Delta S < 0$, van der Waals and hydrogen-bonding interactions play major roles in the reaction. Electrostatic forces are more important when $\Delta H < 0$ and $\Delta S > 0$. If the temperature changes only a little, the enthalpy change (ΔH) can be regarded as a constant.

To obtain such information, the implications of the present result have been discussed in conjunction with thermodynamic characteristics obtained for AHDMAPPC–BSA binding, and the thermodynamic parameters were calculated from the van't Hoff equation,

$$\ln K_T = -\frac{\Delta H}{RT} + \frac{\Delta S}{R} \quad (5)$$

K is the binding constant at temperature T and R is gas constant. The enthalpy change (ΔH) is calculated from the slope of the van't Hoff relationship. The free energy change (ΔG) is estimated from the following relationship:

$$\Delta G^\circ = \Delta H^\circ - T\Delta S^\circ \quad (6)$$

According to the binding constants at the three different temperatures, 300, 310 and 320 K, the thermodynamic parameters were determined from linear van't Hoff plot (Fig. 5) and were presented in Table 3. (The plot of ln K versus $1/T$ gave a straight line according to the van't Hoff equation). According to the values of the thermodynamic parameters (Table 3) for the interaction of the studied pyrimidine compound with BSA, the binding of pyrimidine derivative to BSA is a spontaneous process, as indicated by the negative free energy change (ΔG), accompanied by a positive

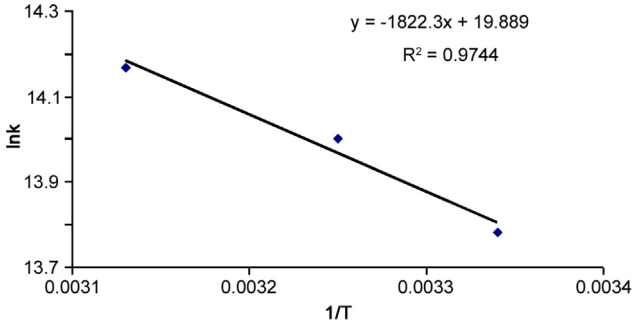

Fig. 5. Van't Hoff plot for the binding of BSA to AHDMAPPC.

Table 3
Thermodynamic parameters of AHDMAPPC–BSA interaction at pH 7.4.

T (K)	ΔH (kJ/mol)	ΔG (kJ/mol)	ΔS (J/mol K)	R
300	15.151	−34.457	165.36	0.9871
310		−36.110		
320		−37.764		

R is the correlation coefficient.

entropy change (ΔS). This binding involves an endothermic reaction as manifested by the positive enthalpy change (ΔH) that is consistent with the increase in K values with temperature.

3.5. Energy transfer between pyrimidine compound and BSA

Energy transfer phenomena have wide applications in the energy conversion process. According to Föster's nonradiative energy transfer theory, the energy transfer will happen under the following conditions: (i) the donor can produce fluorescence light; (ii) the fluorescence emission spectrum of the donor and the UV absorption spectrum of the acceptor have more overlap; and (iii) the distance between the donor and the acceptor is < 8 nm. The overlap of the absorption spectrum of AHDMAPPC with the fluorescence emission spectrum of BSA at pH 7.4 is shown in Fig. 6. The efficiency (E) of energy transfer between the donor and the acceptor can be calculated by the following equations [32]:

$$E = 1 - \frac{F}{F_0} = \frac{R_0^6}{R_0^6 + r^6} \quad (7)$$

where r is the binding distance between donor and receptor, and R_0 is the critical distance when the efficiency of excitation energy transferred to the acceptor is 50%. It can be calculated from donor

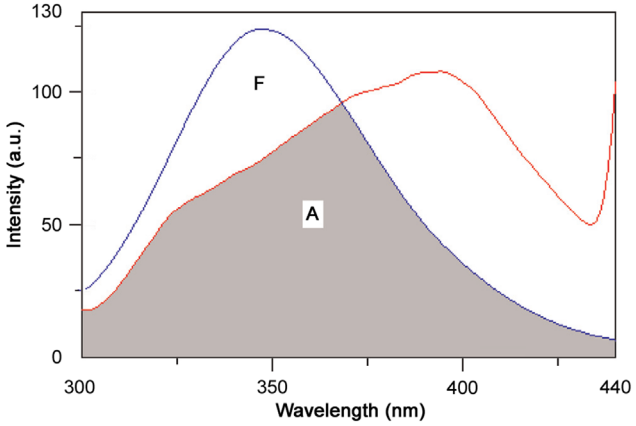

Fig. 6. Spectral overlap of AHDMAPPC excitation (curve A) with BSA emission (curve F). T=300 K, $C_{BSA}=2.0 \times 10^{-5}$ M, $C_{AHDMAPPC}=2.0 \times 10^{-6}$ M.

emission and acceptor absorption spectra using the Föster formula:

$$R_0^6 = 8.79 \times 10^{-25} K^2 n^{-4} \varphi J \quad (8)$$

where K^2 is the spatial orientation factor of the dipole, n is the refractive index of the medium, φ is the fluorescence quantum yield from the donor, and J is the overlap integral of the fluorescence emission spectrum of the donor with the absorption spectrum of the acceptor, which can be calculated by the following equation:

$$J = \frac{\int_0^\infty F(\lambda)\varepsilon(\lambda)\lambda^4 d\lambda}{\int_0^\infty F(\lambda) d\lambda} \quad (9)$$

where $F(\lambda)$ is the fluorescence intensity of the fluorescent donor at a wavelength λ to $\lambda + \Delta\lambda$; and $\varepsilon(\lambda)$ is the molar absorption coefficient of the acceptor at wavelength λ. In the present case $K^2 = 2/3$, $n = 1.336$ and $\varphi = 0.15$ [33]. Hence, from Eqs. (7)–(9), we could calculate that $R_0 = 2.573$ nm, $E = 0.37$ and $r = 2.79$ nm, $r < 7$ nm. The values for R_0 and r are on the 2–8 nm scale and $0.5R_0 < r < 1.5R_0$ indicating an interaction between pyrimidine derivative and BSA (Trp-212). The data suggested that the energy transfer from BSA to AHDMAPPC could occur with high probability. In accordance with prediction by Förster's nonradiative energy transfer theory, these results indicated again a static quenching interaction between pyrimidine derivative and BSA.

3.6. Analysis of the conformation of BSA upon addition of AHDMAPPC

Although it has been confirmed that the binding of pyrimidine derivative to BSA results in the fluorescence quenching of BSA, it is still a puzzle about whether the binding affects the structure and the microenvironment of BSA. Therefore, we utilized the methods of UV–vis absorption, synchronous fluorescence, three-dimensional fluorescence spectroscopy and circular dichroism to further investigate the conformational changes of BSA.

3.6.1. UV–vis absorption spectral studies

UV–vis absorption measurement is a very simple method and applicable to explore the structural changes and to know the complex formation [34,35]. The UV absorption spectrum (Figs. 7 and 8) shows the effect of pyrimidine derivative, AHDMAPPC on the BSA absorption spectrum. As shown in Fig. 8, a strong absorption peak was observed at 279 nm and 390 nm, and the peak intensity increased with the concentration of AHDMAPPC. Furthermore, the formation of AHDMAPPC–BSA complex resulted in a slight shift (from 279 nm to 284 nm) of the spectrum towards longer wavelengths indicating the interaction between pyrimidine derivative and BSA. The presence of isosbestic point also implies the formation of complex.

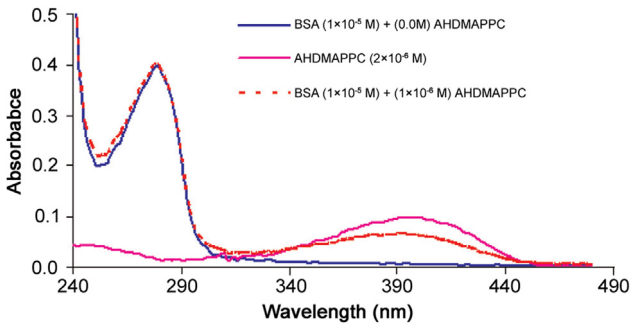

Fig. 7. UV–visible spectra of AHDMAPPC only, AHDMAPPC–BSA 1:1 complex, and BSA only ($T = 300$ K, pH = 7.4).

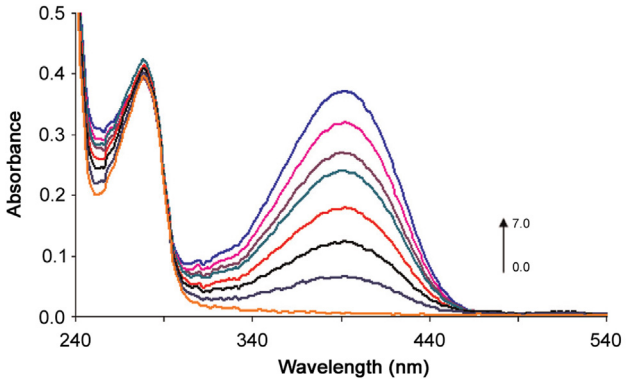

Fig. 8. Effect of AHDMAPPC on the UV–vis absorption of BSA. $C_{BSA} = 1.0 \times 10^{-5}$ M; $C_{AHDMAPPC}(10^{-6}$ M): 0.0, 1.0, 2.0, 3.0, 4.0, 5.0, 6.0, 7.0 ($T = 300$ K, pH = 7.4).

The obvious enhancement of absorbance intensity also indicated the formation of a new complex between them; in addition, the structure of BSA changed upon interaction with AHDMAPPC. The strong absorption peak at around 278 nm is due to the aromatic amino acids (tryptophan, tyrosine and phenylalanine). With gradual addition of AHDMAPPC, the peak intensity of BSA at 278 nm increases with a red shift, which indicated that the interaction between them leads to the loosening and unfolding of the protein backbone and decreases the hydrophobicity of the microenvironment of BSA.

3.6.2. Synchronous fluorescence spectroscopic studies of BSA

Synchronous fluorescence spectroscopy, with several advantages such as sensitivity, spectral simplification, spectral bandwidth, reducing and avoiding different perturbing effects, is a very useful method to study the microenvironment of amino acid residues by measuring the emission wavelength shift and several advantages, such as sensitivity, spectral simplification, spectral bandwidth reduction and avoiding different perturbing effects [36,37]. Miller suggested a useful method to study the environment of amino acid residues by measuring the possible shift in wavelength emission maximum λ_{max}. The shift in position of emission maximum corresponds to the changes of the polarity around the chromophore molecule [38]. As is known, synchronous fluorescence spectra show Trp residues of BSA only at the wavelength interval ($\Delta\lambda$) of 60 nm and Tyr residues of BSA only at $\Delta\lambda$ of 15 nm. Fig. 9 shows the synchronous fluorescence spectra of Trp residues in BSA and those of Tyr residues in BSA with various amounts of pyrimidine derivative, respectively. It can be seen from Fig. 9 that the maximum emission wavelength kept the position at the investigated concentrations range when $\Delta\lambda = 15$ nm while the maximum emission wavelength had a slight blue shift (337 nm → 334 nm) when $\Delta\lambda = 60$ nm. It indicated that the polarity around tryptophan residues decreased, which suggested that tryptophan residue was placed in a more hydrophobic environment. This implies that the interaction of AHDMAPPC with BSA may cause a minor conformational change of Trp residue micro-regions.

3.6.3. Three-dimensional (3D) fluorescence spectra

Three-dimensional fluorescence spectra has become a popular fluorescence analysis technique in recent years. It is well known that three-dimensional fluorescence spectrum can provide more detailed information about the change of the configuration of proteins [39]. In addition, the contour map can also provide a lot of important information. Fig. 10 presents the three-dimensional fluorescence spectra and contour ones of BSA (A) and AHDMAPPC–BSA (B), respectively with the corresponding parameters shown in Table 4. The contour map displays a bird's eye view of the

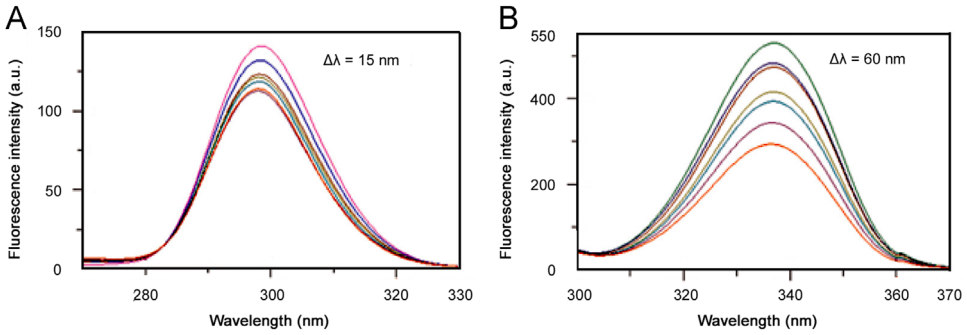

Fig. 9. Synchronous fluorescence spectrum of BSA (T=300 K, pH=7.4, $C_{BSA}=2.0\times10^{-5}$ M, $C_{AHDMAPPC}(10^{-6}$ M): 0, 1.0, 2.0, 3.0, 4.0, 5.0, 6.0). (A) $\Delta\lambda$=15 nm and (B) $\Delta\lambda$=60 nm.

fluorescence spectra. In Fig. 10A, peak A is the Rayleigh scattering peak ($\lambda_{ex}=\lambda_{em}$) and typical fluorescence peaks also can be easily observed in the isometric three-dimensional projection or three-dimensional fluorescence contour map of BSA ($\lambda_{ex}/\lambda_{em}$=260/340 nm). From Fig. 10B, it can be seen that the fluorescence intensity of peak A decreased with the increase of pyrimidine compound, due to the formation of a drug–BSA complex after the addition, making the diameter of BSA decreased, which in turn resulted in the decrease of the scattering effect. As referred to peak B, we think that it mainly reveals the spectral characteristic of tryptophan and tyrosine residues. The reason is that when serum albumin is excited at 280 nm, it mainly reveals the intrinsic fluorescence of tryptophan and tyrosine residues, which is related to changes in the conformation of the peptide backbone associated with the helix-coil transformation. The

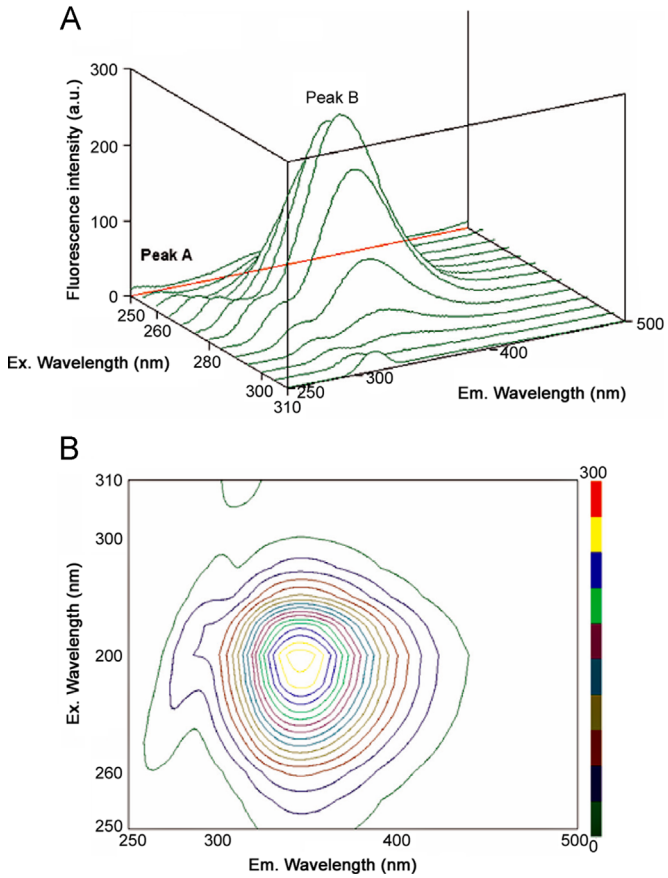

Fig. 10. The three-dimensional projections and the corresponding excitation–emission matrix fluorescence diagrams of BSA before (A) and after (B) AHDMAPPC addition. $C_{BSA}=2.0\times10^{-5}$ M, $C_{AHDMAPPC}=6.0\times10^{-6}$ M, T=300 K, pH=7.4.

fluorescence intensity of the peak decreased markedly following the addition of AHDMAPPC, indicating that the conformations of the peptide backbone, tryptophan and tyrosine residues of BSA were altered. This suggests that the binding of AHDMAPPC–BSA induced some microenvironmental and conformational changes in BSA; a complex between them has been formed.

3.6.4. *Measurement of circular dichroism*

The alterations in the secondary structure of the protein in the presence of the probe were studied by measuring CD on a J-815CD spectrophotometer using a quartz cuvette of path length 0.1 cm at 1 nm data pitch intervals. All CD spectra were taken in a wavelength range 190–250 nm. The spectrophotometer was sufficiently purged with 99.9% nitrogen before starting the instruments. The spectra were collected at a scan speed of 50 nm/min with response time of 1 s at 300 K temperature. Each spectrum was baseline corrected and the final plot was taken as an average of four accumulated plots. The results were expressed as the mean residue ellipticity (MRE in deg cm^2 dmol^{-1} res^{-1}), which is defined by the following equation [40]:

$$\text{MRE} = \frac{ObservedCD\ (\text{m deg})}{C_p \times n \times l \times 10} \tag{10}$$

where n is the number of amino acid residues (583 for BSA), l is the path length of the cell (0.1 cm), and C_p is the protein concentration in moles dm^{-1}. Helicity content was calculated from the MRE values at 222 nm using the following equation [40]:

$$\%\alpha\text{-helix}(\%) = \frac{-(MRE_{222} - 2340)}{30300} \times 100 \tag{11}$$

Far UV CD spectra were recorded to examine the secondary structure of BSA in the presence of AHDMAPPC. Fig. 11 shows the CD spectra of free BSA and BSA – AHDMAPPC complex. As seen in Fig. 11, BSA and its complex with probe exhibit negative absorption bands with maxima at ~208 nm ($n\rightarrow\pi^*$) and 222 nm ($\pi\rightarrow\pi^*$), which are the characteristic band of the α-helical structure of BSA [41–44]. In presence of AHDMAPPC, we observed that the intensity of the negative band increased without any discernible shift of the band maxima. This increase in ellipticity indicates stabilization of the complex with respect to free BSA [40]. We also calculated the percentage of α-helix by using Eqs. (10) and (11) for free BSA and BSA in the presence of AHDMAPPC. From these calculations, we found that α-helical content of BSA increased from 56.4% for free BSA to 58.6% at a molar ratio AHDMAPPC:BSA of 1:1 and to 66.3% at 1:4 concentration upon binding to BSA. Such slight changes in α-helical content of BSA, upon binding with small ligands, are consistent with reported literature [45–49].

Table 4
Three-dimensional fluorescence spectral characteristics of BSA and BSA-AHDMAPPC system.

Peaks	BSA			BSA-AHDMAPPC		
	Peak position $\lambda_{ex}/\lambda_{em}$ (nm/nm)	Stokes $\Delta\lambda$ (nm)	Intensity (F)	Peak position $\lambda_{ex}/\lambda_{em}$ (nm/nm)	Stokes $\Delta\lambda$ (nm)	Intensity (F)
Rayleigh scattering peaks	280/280	0	83.6	280/280	0	64.3
Fluorescence peaks	280/342	62	273.1	280/344	64	118.7

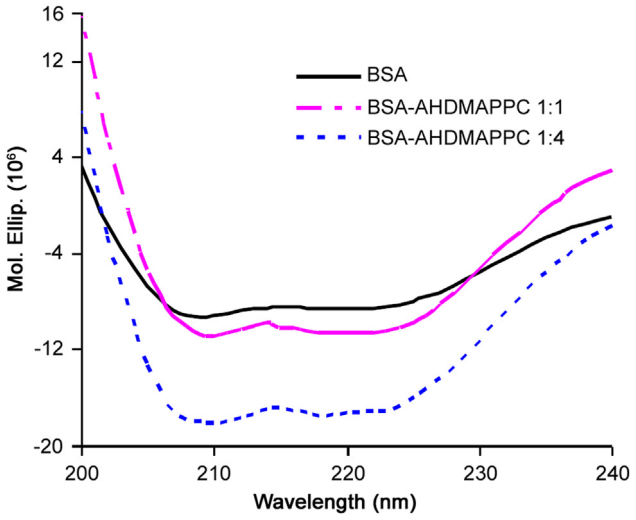

Fig. 11. Circular dichroism spectra of free BSA and AHDMAPPC–BSA complexes. $C_{BSA}=2.0\times10^{-5}$ M, $C_{AHDMAPPC}=2.0\times10^{-6}$ M, $T=300$ K, pH=7.4.

4. Conclusions

Binding interaction of a biologically active pyrimidine derivative with BSA was investigated in detail using different spectroscopic methods. We used different approaches to explore the interactions under physiological conditions. The experimental results showed that the fluorescence quenching of model carrier protein, BSA, by reagent was a result of the formation of complex between them by static quenching. The site binding constants and number of binding sites were determined at three different temperatures. The thermodynamic parameters indicated that the reaction was endothermic and spontaneous process, and hydrophobic interactions played a major role in the binding of drug to BSA. The distance between donor and acceptor and alterations of BSA secondary structure in the presence of pyrimidine derivative were also confirmed. All these experimental results and theoretical data clarified that pyrimidine derivative can bind to BSA and be effectively transported and eliminated, which can be a useful guideline for further clinical study.

Acknowledgments

The author (VDS) gratefully acknowledges receiving a fellowship from UGC, New Delhi [University Grant Commission, the XIth plan (Faculty Improvement Programme)] and thanks to DST and UGC for providing funds to the department under FIST and SAP programme.

References

[1] P.B. Kandagal, S. Ashoka, J. Seetharamappa, et al., Study of the interaction of an anticancer drug with human and bovine serum albumin: spectroscopic approach, J. Pharm. Biomed. Anal. 41 (2006) 393–399.
[2] X. Zhu, J. Sun, Y. Hu, Determination of protein by hydroxypropyl-b-cyclodextrin sensitized fluorescence quenching method with erythrosine sodium as fluorescence probe, Anal. Chim. Acta 596 (2007) 298–302.
[3] V.D. Suryawanshi, P.V. Anbhule, A.H. Gore, et al., Spectroscopic investigation on the interaction of pyrimidine derivative, 2-amino-6-hydroxy-4-(3,4 dimethoxyphenyl)-pyrimidine-5-carbonitrile with human serum albumin: mechanistic and conformational study, Ind. Eng. Chem. Res. 51 (2012) 95–102.
[4] T. Peters, All about Albumin: Biochemistry, Genetics and Medical Application, Academic Press, New York, 1996.
[5] X.M. He, D.C. Carter, Atomic structure and chemistry of human serum albumin, Nature 358 (1992) 209–215.
[6] U.S. Mote, S.L. Bhattar, S.R. Patil, et al., Interaction between felodipine and bovine serum albumin: fluorescence quenching study, Luminescence 25 (2010) 1–8.
[7] Y.Q. Wang, H.M. Zhang, G.C. Zhang, et al., Spectroscopic studies on the interaction between silicotungstic acid and bovine serum albumin, J. Pharm. Biomed. Anal. 43 (2007) 1869–1875.
[8] V. Anbazhagan, R. Renganathan, Study on the binding of 2,3-diazabicyclo [2.2.2]oct-2-ene with bovine serum albumin by fluorescence spectroscopy, J. Lumin. 128 (2008) 1454–1458.
[9] Y. Moriyama, D. Ohta, K. Hadiya, et al., Fluorescence behavior of tryptophan residues of bovine and human serum albumins in ionic surfactant solutions: a comparative study of the two and one tryptophan(s) of bovine and human albumins, J. Protein Chem. 15 (1996) 265–272.
[10] G.N. Pershin, L.I. Sherbakova, T.N. Zykova, et al., Antibacterial activity of pyrimidine and pyrrolo-(3,2-d)-pyrimidine derivatives, Farmakol. Taksikol. 35 (1972) 466–471.
[11] G. Regnier, R. Canevari, J. Le Douarec, et al., Triphenylpropylpiperazine derivatives as new potent analgetic substances, J. Med. Chem. 15 (1972) 295–298.
[12] S. Saeed, N. Rashid, P.G. Jones, et al., Synthesis and pharmacological properties of N-substituted-N′-(4,6-dimethylpyrimidin-2-yl)-thiourea derivatives and related fused heterocyclic compounds, J. Heterocycl. Chem. 48 (2011) 74–82.
[13] K. Suguira, A.F. Schmid, M.M. Schmid, et al., Effect of compounds on a spectrum of rat tumors, Cancer Chemother. Rep. Part 23 (1973) 231–233.
[14] U. Kragh-Hansen, Molecular aspects of ligand binding to serum albumin, Pharmacol. Rev. 33 (1981) 17–53.
[15] M.B. Deshmukh, S.M. Salunkhe, D.R. Patil, et al., A novel and efficient one step synthesis of 2-amino-5-cyano-6-hydroxy-4-aryl pyrimidines and their antibacterial activity, Eur. J. Med. Chem. 44 (2009) 2651–2654.
[16] A. Kathiravan, M. Chandramohan, R. Renganathan, et al., Spectroscopic studies on the interaction between phycocyanin and bovine serum albumin, J. Mol. Struct. 919 (2009) 210–214.
[17] G. Colmenarejo, In silico prediction of drug-binding strengths to human serum albumin, Med. Res. Rev. 23 (2003) 275–301.
[18] A. Papadopoulou, R.J. Green, R.A. Frazier, Interaction of flavonoids with bovine serum albumin: a fluorescence quenching study, J. Agric. Food Chem. 53 (2005) 158–163.
[19] Z. Chi, R. Liu, Y. Teng, et al., Binding of oxytetracycline to bovine serum albumin: spectroscopic and molecular modeling investigations, J. Agric. Food Chem. 58 (2010) 10262–10269.
[20] G.Z. Chen, X.Z. Huang, J.G. Xu, Fluorimetry, second ed., Science Press, Beijing, 1990, pp. 122.
[21] G. Paramaguru, A. Kathiravan, S. Selvaraj, et al., Interaction of anthraquinone dyes with lysozyme: evidences from spectroscopic and docking studies, J. Hazard. Mater. 175 (2010) 985–991.
[22] J.R. Lakowicz, Principles of Fluorescence Spectroscopy, third ed., Springer, New York, 2006.
[23] J.R. Lakowicz, Principles of Fluorescence Spectroscopy, second ed., Springer, Kluwer Academic/Plenum, New York, 1999.
[24] X. Zhao, R. Liu, Z. Chi, et al., New insights into the behavior of bovine serum albumin adsorbed onto carbon nanotubes: comprehensive spectroscopic studies, J. Phys. Chem. B 114 (2010) 5625–5631.
[25] Y.J. Hu, Y.O. Yang, C.M. Dai, et al., Binding of berberine to bovine serum albumin: spectroscopic approach, Mol. Biol. Rep. 37 (2010) 3827–3832.
[26] W.R. Ware, Oxygen quenching of fluorescence in solution: an experimental study of diffusion process, J. Phys. Chem. 66 (1962) 455–458.
[27] S.S. Lehrer, Solute perturbation of protein fluorescence. Quenching of the tryptophyl fluorescence of model compounds and of lysozyme by iodide ion, Biochemistry 10 (1971) 3254–3263.
[28] L. Zhao, R. Liu, X. Zhao, et al., New strategy for the evaluation of CdTe quantum dot toxicity targeted to bovine serum albumin, Sci. Total Environ. 407 (2009)

5019–5023.
[29] G. Colmenarejo, A. Alvarez-Pedraglio, J.L. Lavandera, Cheminformatic models to predict binding affinities to human serum albumin, J. Med. Chem. 44 (2001) 4370–4378.
[30] C. Dufour, O. Dangles, Flavonoid-serum albumin complexation: determination of binding constants and binding sites by fluorescence spectroscopy, Biochim. Biophys. Acta 2005 (1721) 164–173.
[31] P.D. Ross, S. Subramanian, Thermodynamics of protein association reactions: forces contributing stability, Biochemistry 20 (1981) 3096–3102.
[32] Z. Chi, R. Liu, H. Zhang, Noncovalent interaction of oxytetracycline with the enzyme trypsin, Biomacromolecules 11 (2010) 2454–2459.
[33] Y.J. Hu, Y. Liu, X.H. Xiao, Investigation of the interaction between berberine and human serum albumin, Biomacromolecules 10 (2009) 517–521.
[34] X. Pan, P. Qin, R. Liu, et al., Characterizing the interaction between tartrazine and two serum albumins by a hybrid spectroscopic approach, J. Agric. Food Chem. 59 (2011) 6650–6656.
[35] B. Valeur, Molecular Fluorescence: Principles and Applications, Wiley-VCH Press, New York, 2001.
[36] S.Y. Bi, D.Q. Song, Y. Tian, et al., Molecular spectroscopic study on the interaction of tetracyclines with serum albumins, Spectrochim. Acta Part A 61 (2005) 629–636.
[37] D. Li, M. Zhu, C. Xu, et al., Characterization of the baicalein-bovine serum albumin complex without or with Cu^{2+}or Fe^{3+} by spectroscopic approaches, Eur. J. Med. Chem. 46 (2011) 588–599.
[38] G.Z. Chen, X.Z. Huang, Z.Z. Zheng, et al., Fluorescence Analytical Method. second ed., Science Press, Beijing, 1990, pp. 117.
[39] J.B.F. Lloyd, I.W. Evett, Prediction of peak wavelengths and intensities in synchronously excited fluorescence emission spectra, Anal. Chem. 49 (1977) 1710–1715.
[40] J.N. Miller, Recent advances in molecular luminescence analysis, Proc. Anal. Div. Chem. Soc. 16 (1979) 203–208.
[41] F. Ding, W. Liu, J.X. Diao, et al., Characterization of Alizarin Red S binding sites and structural changes on human serum albumin: a biophysical study, J. Hazard. Mater. 186 (2010) 352–359.
[42] D. Sarkar, A. Mahata, P. Das, et al., Deciphering the perturbation of serum albumins by a ketocyanine dye: a spectroscopic approach, J. Photochem. Photobiol. B 96 (2009) 136–143.
[43] A. Chakrabarty, A. Mallick, B. Haldar, et al., Binding interaction of a biological photosensitizer with serum albumins: a biophysical study, Biomacromolecules 8 (2007) 920–927.
[44] M.G. Gore, Spectrophotometry and Spectrofluorimetry: A Practical Approach, third ed., Oxford University Press, Oxford, UK, 2000.
[45] B. Ahmad, S. Parveen, R.H. Khan, Effect of albumin conformation on the binding of ciprofloxacin to human serum albumin: a novel approach directly assigning binding site, Biomacromolecules 7 (2006) 1350–1356.
[46] Y. Moriyama, K. Takeda, Re-formation of the helical structure of human serum albumin by the addition of small amounts of sodium dodecyl sulfate after the disruption of the structure by urea. A comparison with bovine serum albumin, Langmuir 15 (1999) 2003–2008.
[47] T.K. Maiti, K.S. Ghosh, J. Debnath, et al., Binding of all-trans retinoic acid to human serum albumin: fluorescence, FT-IR and circular dichroism studies, Int. J. Biol. Macromol. 38 (2006) 197–202.
[48] N. Ibrahim, H. Ibrahim, S. Kim, et al., Interactions between antimalarial indolone-N-oxide derivatives and human serum albumin, Biomacromolecules 11 (2010) 3341–3351.
[49] X.F. Zhang, L. Xie, Y. Liu, et al., Molecular interaction and energy transfer between human serum albumin and bioactive component Aloe dihydrocoumarin, J. Mol. Struct. 888 (2008) 145–151.